Arabian Journal of Chemistry (2022) **15**, 104060

King Saud University

Arabian Journal of Chemistry

www.ksu.edu.sa
www.sciencedirect.com

ORIGINAL ARTICLE

Synthesis of novel nano-radiotracer for in-vivo bone imaging: ^{99m}Tc- citric acid based PEG dendrimer and its conjugation with alendronate

Behnam davoodikia [a], Morteza Pirali Hamedani [b], Mostafa Saffari [c], Seyed Esmaeil Sadat Ebrahimi [b], Mohammad Seyyed hamzeh [b], Shaghayegh Hashemi [b,*], Mehdi Shafiee Ardestani [b,*], Seyedeh Masoumeh Ghoreishi [d,*]

[a] *School of pharmacy international campus Tehran university of medical sciences, Tehran, Iran*
[b] *Department of Radiopharmacy, Faculty of Pharmacy, Tehran University of Medical Sciences, Tehran, Iran*
[c] *Branch of Pharmaceutical Sciences, Islamic Azad University, Tehran, Iran.Department of Pharmaceutics & Medical Nanotechnology*
[d] *Cellular and Molecular Biology Research Center, Health Research Institute, Babol University of Medical Sciences, Babol, Iran*

Received 12 April 2022; accepted 16 June 2022
Available online 20 June 2022

KEYWORDS

Citric acid dendrimer;
Alendronate;
Bone scan;
Radiolabeling;
SPECT;
MDP

Abstract Bone scan is the test that guide physician to diagnose diseases in the bone at the early stage, to prevent metastases to other organs. In this study, citric acid dendrimer conjugation with alendronate was synthesized. Obtained product was confirmed by FT-IR and TEM. Cytotoxicity assay at different concentrations showed no toxicity on normal cell line compared to control group. Radiolabeling process was optimized by Box-Behnken software which is a computational method to determine optimum of important radiolabeling parameters. Optimized parameter for reducing agent, dendrimer-G_2-alendronate, and time for shaking was 1 mg, 12.3 mg, and 25 min respectively. For determination of in-vivo accumulation of ^{99m}Tc-dendrimer-G_2-alendronate, SPECT imaging was done. Images showed high accumulation of radio-tracer in the skeletal compared to ^{99m}Tc-MDP which is the frequent bone scan agent. All in all, obtained results confirmed our hypothesis

* Corresponding authors.
E-mail addresses: shaghayeghh1374@yahoo.com (S. Hashemi), Shafieeardestani@gmail.com (M. Shafiee Ardestani), M.ghoreishi@mubabol.ac.ir (S. Masoumeh Ghoreishi).
Peer review under responsibility of King Saud University.

Production and hosting by Elsevier

https://doi.org/10.1016/j.arabjc.2022.104060

that the dendrimer-G_2-alendronate can be noteworthy nano-radiopharmaceuticals to bone cancer imaging at early stage.

1. Introduction

Nanotechnology is a field that manipulates materials to design and produce structures in a nanometer scale. Nanomaterials named materials in the range of 1–100 nm at least in one dimension (Sim and Wong, 2021; Patra et al., 2018). Nanotechnology entered in many fields of sciences, including biotechnology, medicine, textile, engineering, and so on (Shirzadi-Ahodashti et al., 2020; Ebrahimzadeh et al., 2021; Ahmadi et al., 2020). The entering nanomaterials into medicine named ''nano-medicine" have fascinated researchers in the wide range of applications from imaging agents to delivery systems (Shirzadi-Ahodashti et al., 2020; Murthy, 2007; Shirzadi-Ahodashti et al., 2020; Naghizadeh et al., 2021). The small particle size of nanomaterials allows them to penetrate through the biological barriers, and high therapeutic efficiency will be achieved (Su and Kang, 2020). In addition, solubility and bioavailability will be improved by nano-carrier systems. Many medicines based nanomaterials have entered the clinic, and there are enormous nanomedicines candidates for FDA approval (Ventola, 2017; Resnik and Tinkle, 2007).

Among different kinds of nanoparticles, dendrimers have attracted consideration due to the conjugation ability on the surface and trapping inside the dendrimer (Barrett et al., 2009; Svenson and Tomalia, 2005). Studies showed that many dendrimers reveal toxicity in vivo through the cell wall interaction and the surface modification by polyethylene glycol (PEG) or citric acid reduce the toxicity (Jain et al., 2010). In this study, synthesized dendrimer consists of PEG as a core and citric acid as branches that introduce a non-toxic dendrimer for in vivo evaluation.

Since, imaging techniques that diagnose diseases at the early stage have an important role in the prevention and treatment of diseases, designing the tracers which detect the diseases more precisely is essential. Molecular imaging is a non-invasive technique that provides useful information at the molecular and cellular levels. This procedure is based on physiological changes determined by the uptake of radiotracer in the target-specific organ. Thus, investigating new radiotracers for diagnosis of diseases more accurately is still a critical issue (Wu and Shu, 2018; Gomes et al., 2011).

Alendronate is a bisphosphonate drug used to treat and prevent osteoporosis and Paget's disease of bone. Its mechanism is through the inhibition of osteoclastic bone resorption (Porras et al., 1999). Due to the structure and application of alendronate, in this study, alendronate was used in nanoscale to target the bone. Scanning the bone is the test in which helps physicians to diagnose bone disorders at early stage, especially for finding cancer that has started or metastatic to bone (Heindel et al., 2014). Although, bisphosphonates kits were used frequently in nuclear medicine as bone imaging agents (Simon et al., 1990; Davis and Jones, 1976), research on imaging tracers that detect bone disorders more accurately is still required. In this framework, *Ren et al*, designed the gadolinium-labeled luminescent mesoporous silica nanoparticles and dexamethasone loaded into nanocarrier. The results showed the sustained release behavior of dexamethasone. Also, they claim that it can be used as a potential magnetic contrast agent (Ren et al., 2017). *Patricio et al*, synthesized the PLA/PVA/EDTMP polymeric nanoparticles and labeled with technetium-99 m for in-vivo evaluation. Results showed that the polymeric nanoparticles are suitable carriers and showed phosphor prolonged release for EDTMP (Patricio et al., 2014).

In this study, we synthesized the nano-radiotracer for the bone scan. Second-generation dendrimer based on the citric acid, was conjugated to the alendronate as a targeting agent. Since, the methylene diphosphonate (MDP) kit is used frequently as a bone imaging agent in the nuclear medicine centers, we used this radiophamaceuticals as a control group, and the results were compared with nano-radiotracer. Although, many studies need to be done for further investigation of this nano-radiotracer, our result showed that the nano-radiotracer showed bone accumulation more than ^{99m}Tc-MDP.

2. Material and method

All chemical reagents were of analytical grade and used without further purification. Citric acid, polyethylene glycol (PEG), N,N′-Dicyclohexylcarbodiimide (DCC), 1-Ethyl-3-(3-dimethylaminopropyl)carbodiimide (EDC), alendronate, and N-Hydroxysuccinimide (NHS) were purchased from Merck. Dimethylformamide (DMF), stannous chloride ($SnCl_2$), MTT kit, and dialysis bag (molecular weight cut-off 500 Da) were purchased from Sigma. HEK-293 cell line was prepared from Pasteur Institute (Tehran, Islamic Republic of Iran). Fourier Transform Infrared spectroscopy (FT-IR) of the powders by making KBr pellet acquired using Perkin Elmer Spectrum BX-II spectrometer. Transmission electron microscopy (TEM) images were investigated using transmission electron microscopy (TEM, JEM-2100). SPECT images were done by Siemens, SimbiaT2 equipped with LEHR collimators instrument. Studies were directed in line with the principles of the declaration of Tehran University of medical sciences with the number: IR.TUMS.TIPS.REC.1399.166.

2.1. Synthesis

Dendrimer-G_2 was synthesized based on our previous study (Ardestani et al., 2020). Briefly, 2 mL PEG was dissolved in 10 mL DMF in the presence of 7.4 mmol (1.5 g) DCC. The solution stirred for 25 min and after that 4.7 mmol (1.4 g) citric acid was added. The first generation of dendrimer was prepared after one day. The reaction was stopped by addition of distilled water and purified by dialysis bag. The second generation of dendrimer was synthesized in the presence of DCC (1.5 g) and citric acid (1.4 g) (both 2.22 mmol) in the 10 mL DMF and stirred for one day. After stopping the reaction by distilled water, purification was done by dialysis bag. For alendronate conjugation, 20 mg obtained dendrimer-G_2 was dissolved in 4 mL DMF in the presence of EDC, NHS (0.02, 0.01 mmol respectively) and stirred for 30 min. After the pH reached 9 by phosphate buffered saline (PBS), alendronate (20 mg) was added and stirred for one week. Purification was done with dialysis bag. FT-IR, TEM, and EDS were done to confirm production of the final product.

2.2. MTT cytotoxicity assay

MTT is a quantitative colorimetric assay for cell viability evaluation. This assay is based on the reducing tetrazolium (MTT) to insoluble formazan by viable mitochondria. Typically, 10^4

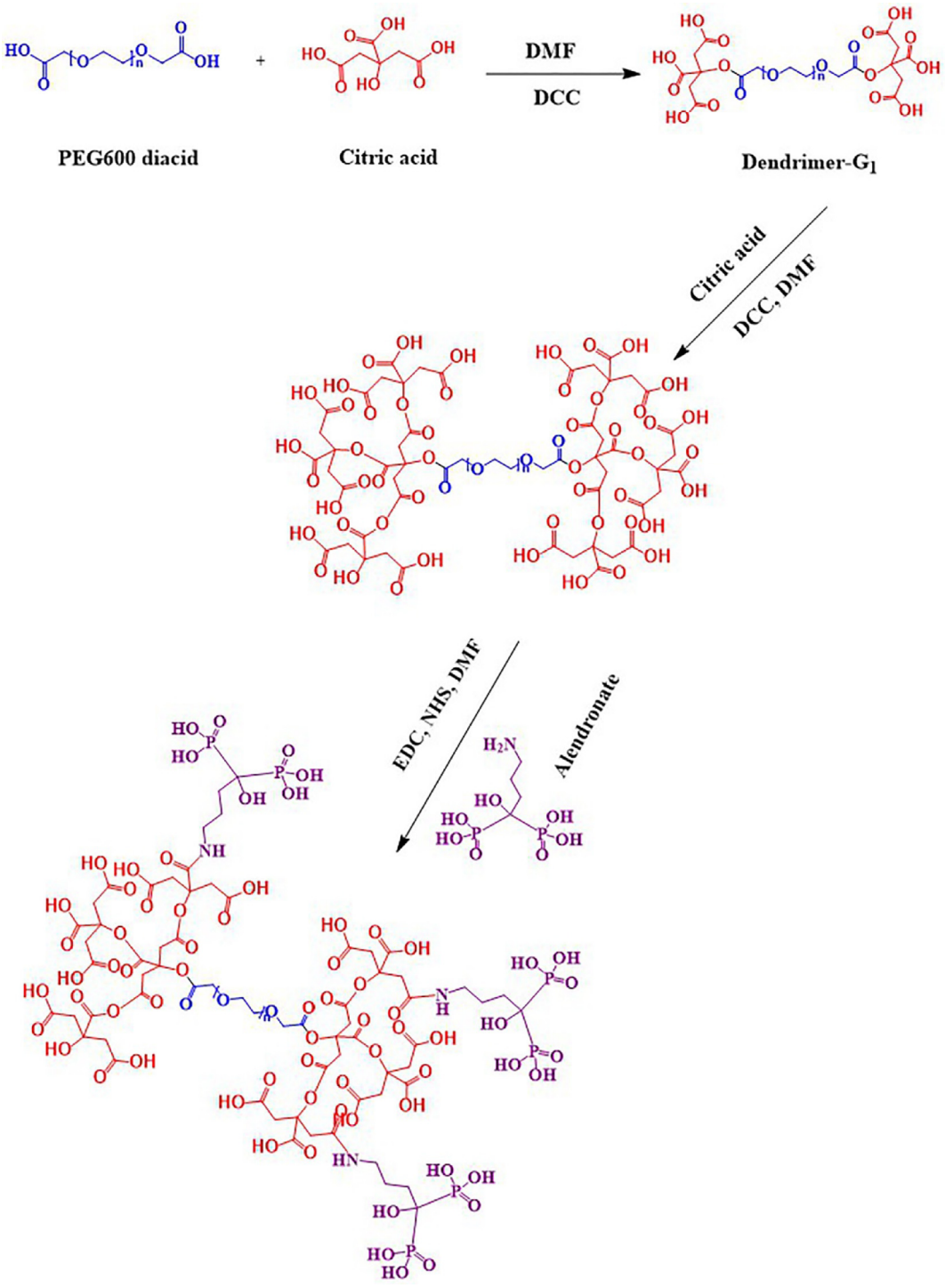

Fig. 1 Schematic illustration of citric acid second generation and conjugation with alendronate.

of HEK-293 cell lines were seeded on a 96-well microplate, and incubated for 24 h at 37 °C. Then, 10 µl of the media (RPMI) was removed, and 10 µl of prepared solution (5 mg of MTT powder in 1 mL of PBS) was added to each well and was incubated for 4 h. Finally, media of each well was removed and DMSO was added. Absorption was read at 570 nm by an enzyme-linked immunosorbent assay (ELISA) reader.

2.3. Radiolabeling

In this study, each factor which plays an important role in the radiolabeling was optimized by Box-Behnken software. Elimination of oxygen, devastating the radiolabeling a lyophilized kit was prepared. For kit preparation, 1 mg/mL (tin chloride/

HCl) was added in dendrimer-G_2-alendronate (12.3 mg/mL) and acid ascorbic (1.8 mg/mL as an antioxidant agent) solution. After adjusting pH to 7, for reducing the effect of oxygen on technetium-99 m labeling yield prepared kit was lyophilized. For radiolabeling, $^{99m}TcO_4^-$ (300 MBq) was eluted from $^{99}Mo/^{99m}Tc$ generator and added to the lyophilized kit and was shaken for about 25 min at room temperature.

2.4. Radiochemical purity

Rapid and simple method was done for radiochemical purity (RCP) determination. According to our previous study (Ardestani et al., 2020); the chromatography method was used for evaluation of radiochemical purity (RCP) of the radiolabeled citric acid dendrimer. This method is a suitable method for time-consuming experiments to save time (Amin et al., 1997). Two different mobile phases, including acetone/methanol (1:1), and saline were chosen and the Whatman paper was chosen as a solid phase. 5 µl samples were spotted at the origin of the paper (1.2 cm × 10 cm). After developing the strip in the solvent, the strip was divided into two parts, and the radioactivity in each part was accounted with a gamma well-type counter. Using acetone/methanol as a mobile phase, $^{99m}TcO_2$ and ^{99m}Tc-dendrimer-G_2-alendronate remain in the origin, and free pertechnetate move with solvent. Thus, the percentage of free pertechnetate was determined. By using saline as mobile phase, $^{99m}TcO_2$ remains in the origin and free pertechnetate and ^{99m}Tc-dendrimer-G_2-alendronate move with solvent. Then, the percentage of $^{99m}TcO_2$ was calculated. Finally, radiochemical purity was evaluated by the following formula: RCP = 100 – (free pertechnetate + $^{99m}TcO_2$) (1).

2.5. SPECT imaging and biodistribution study

Scintigraphy imaging confirmed our hypothesis that ^{99m}Tc-dendrimer-G_2-alendronate is a promising agent for a bone scan. For comparison, the MDP kit, which is regularly used in the nuclear medicine center, was injected as same as ^{99m}Tc-dendrimer-G_2-alendronate as a control group. All groups consist of three mice. 37 MBq of ^{99m}Tc-dendrimer-G_2-alendronate and ^{99m}Tc-MDP were injected through the tail vein. After that, each mouse was placed under SPECT/CT instrument after anesthesia by intraperitoneal injection of ketamine/xylazine. Imaging was acquired after 2 h of injection

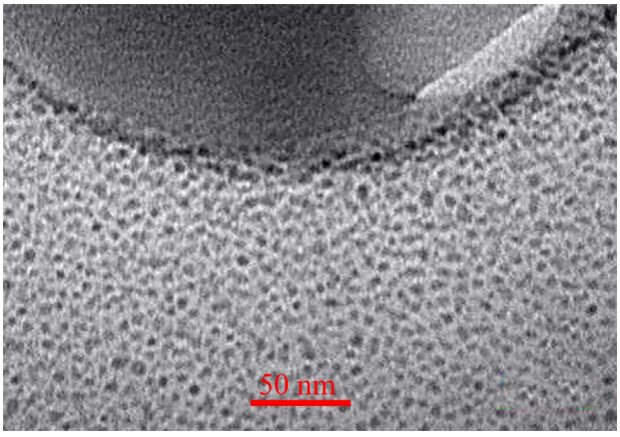

Fig. 3 TEM spectrum of dendrimer-G_2-alendronate.

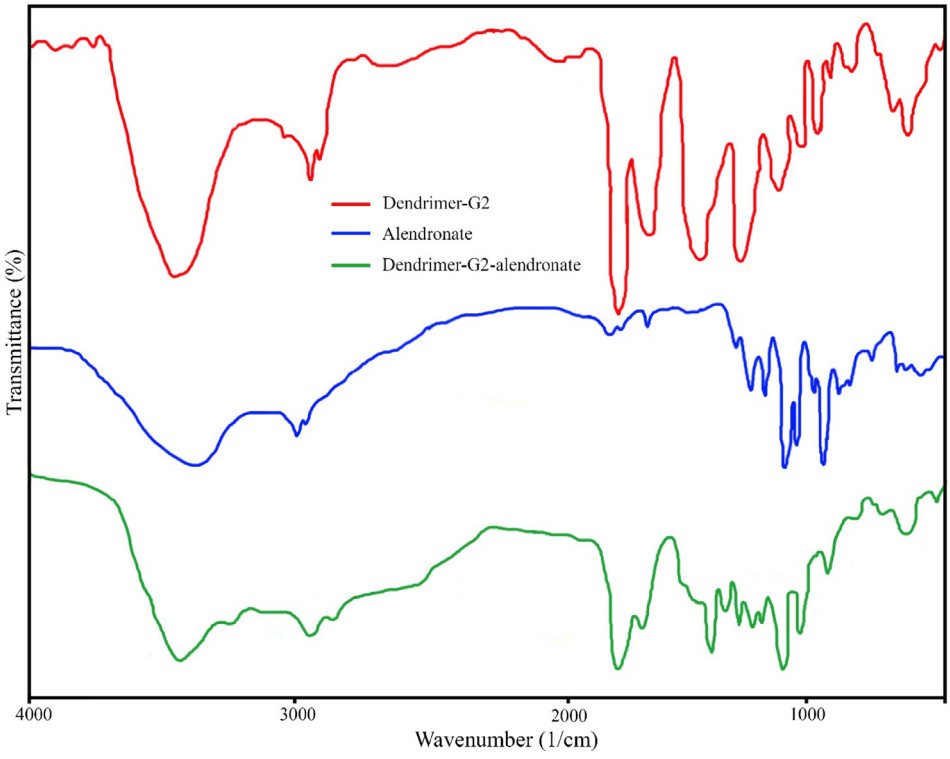

Fig. 2 FT-IR spectrum of dendrimer-G_2 (red), dendrimer-G_2-alendronate (blue), and pure alendronate (green).

using a 256 * 256 matrix size with a 20% energy window set at 140 keV. Accumulation of ^{99m}Tc-dendrimer-G_2-alendronate and ^{99m}Tc-MDP in the targeted organs was presented by hot spot color. Each mouse was sacrificed after SPECT imaging, and different organs were removed. For clearance the surface from blood, organs were washed with normal saline. Blood was collected by cardiac puncture, and activity in each organ was estimated with a gamma well counter. The percentage dose of radioactivity in each organ was evaluated from activities counted (dose per gram of tissue) in each organ divided by total activities.

2.6. Statistical analysis

Statistical analysis was done using Prism 9 and Excel software (Microsoft office 2013). For quantitative data, one-way analysis variance followed by Turkey's test was done. $P < 0.05$ was considered statistically significant.

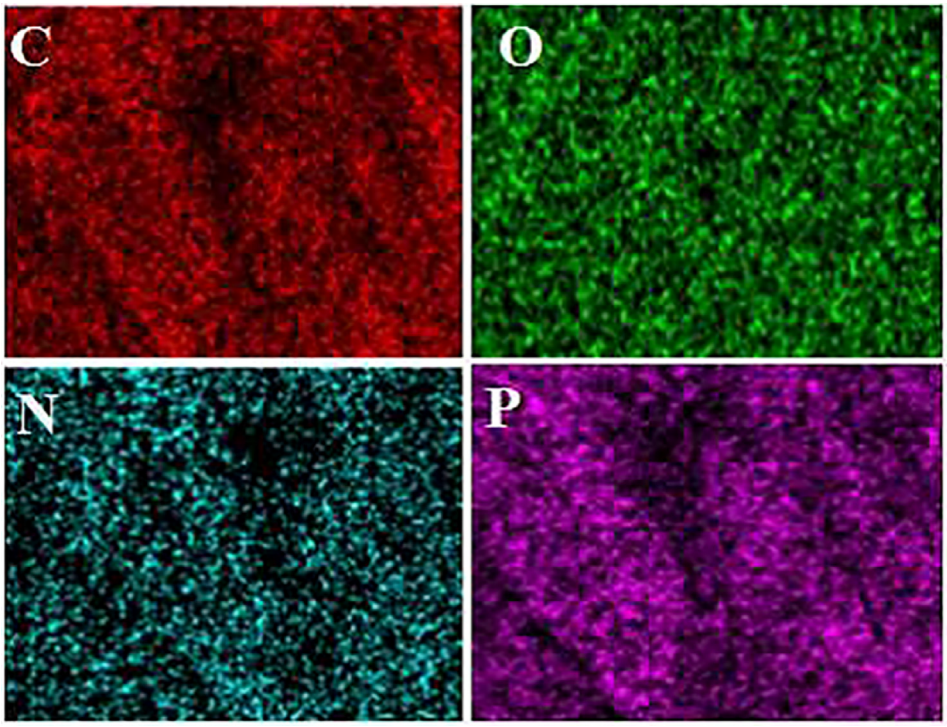

Fig. 4 EDS mapping analysis of dendrimer-G2-alendronate. The mapping confirmed the existence of carbon (C), oxygen (O), nitrogen (N), and phosphorous (P).

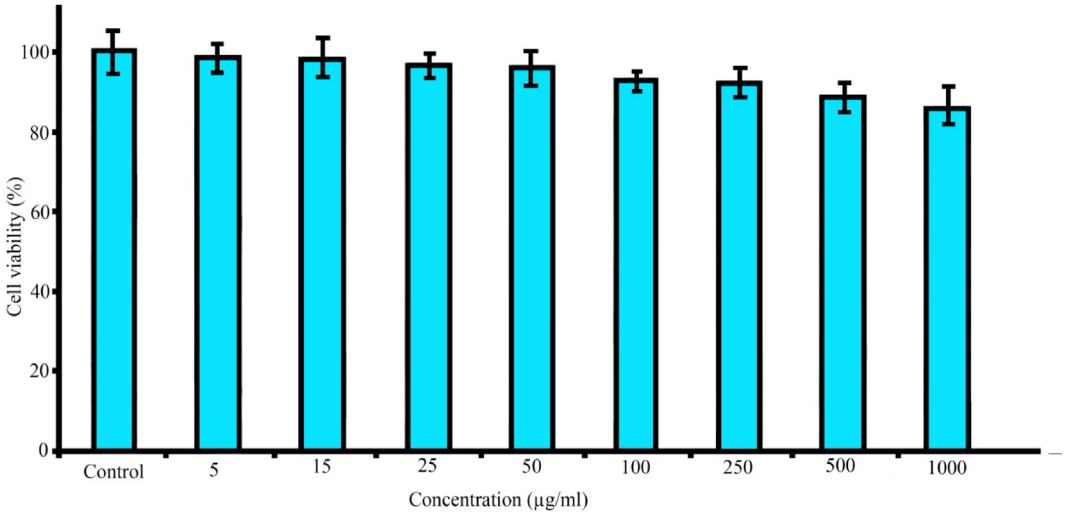

Fig. 5 Cytotoxicity assay of dendrimer-G_2-alendronate on HEK-293 cell line after 24 h at different concentrations.

Table 1 (a). different parameters which effect the radiolabeling including time, amount of reducing agent and dendrimer-G_2-alendronate. (b). Optimal amount of variables that affect radiolabeling.

a: Different parameters which effect the radiolabeling					
Factor	Name	Unit	−1	0	1
A	Time	min	5	20	35
B	Reducing Agent	mg	1	2.5	4
C	Probe	mg	10	15	20
b: Optimal amount of variables					
Time	Reducing Agent (mg)		Probe (mg)	Max Response	
25	1		12.3	94.37	

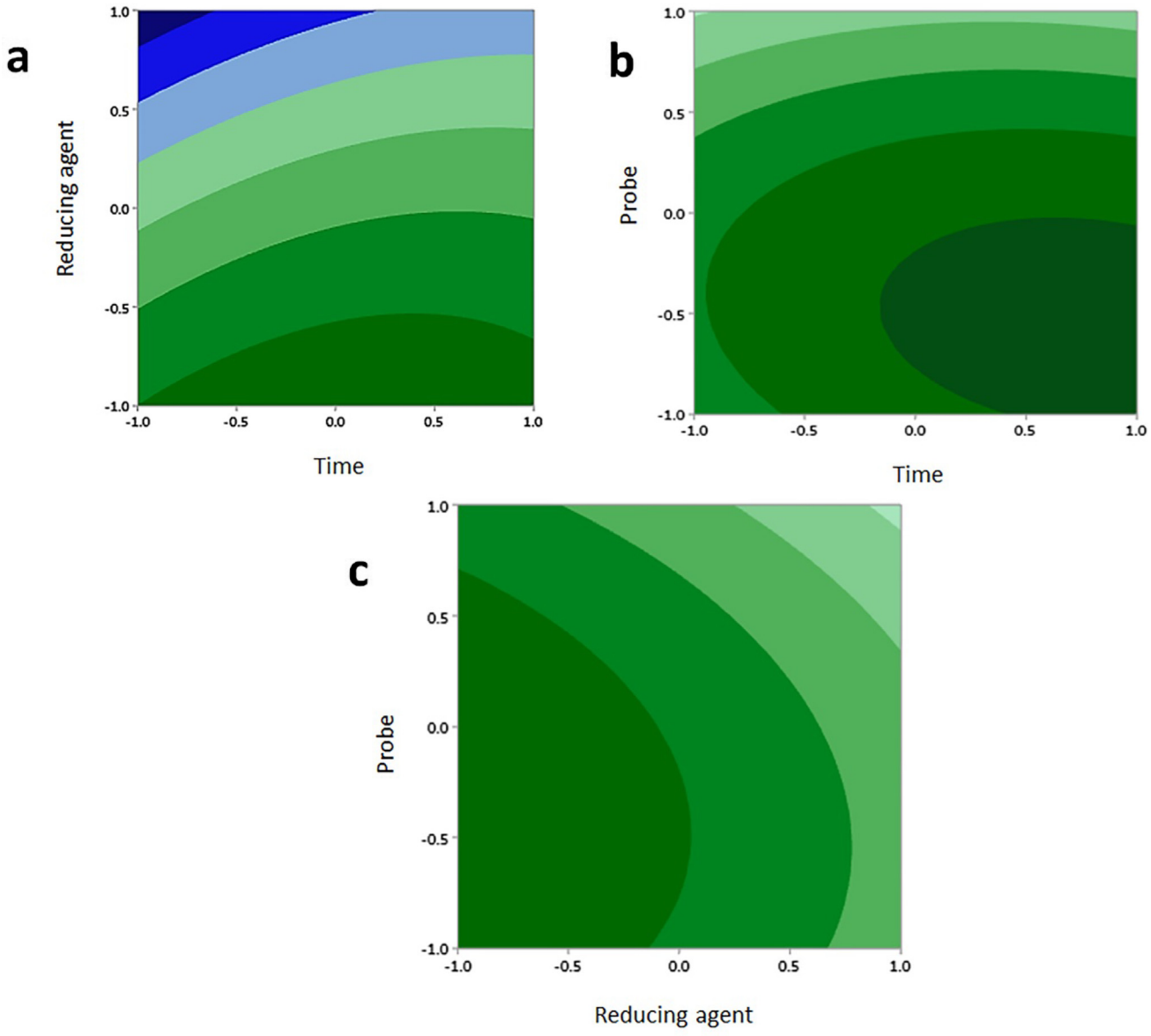

Fig. 6 2D and 3D images effect of two term interactions in average mean of third term. (a) interaction between time & reducing agent, (b) interaction between dendrimer-alendronate & time, (c) interaction between reducing dendrimer-G_2-alendronate & reducing agent. In each term variation is indicated by variation in color.

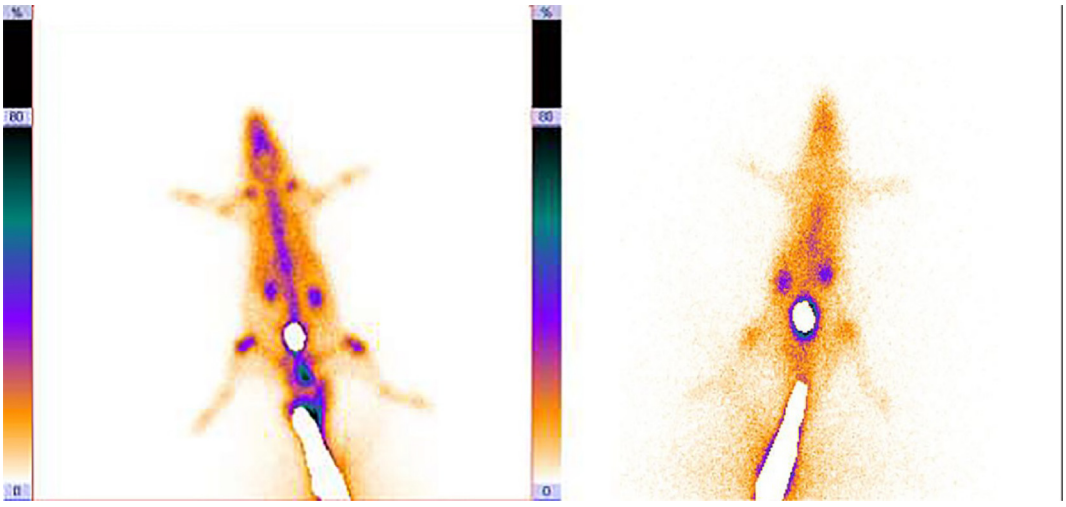

Fig. 7 SPECT imaging of ^{99m}Tc-dendrimer-G_2-alendronate (left), and ^{99m}Tc-MDP (right).

3. Result and discussion

Nanotechnology has been entered in medicine to solve the problems for detection and treatment of diseases. Drug delivery based nanomaterials may change the prospect of pharmaceutical and biotechnology companies (Ciobanu et al., 2011). Thus, research on nanomedicine is still fascinated. Studies claimed that it is possible to designed and developed nanoradiopharmaceuticals for bone imaging. Oliveira & coworkers developed the nanohydroxyapatite labelled with technetium-99 m for bone cancer imaging. They stated that nanoradiopharmaceuticals may change the global history of oncology and nuclear medicine especially for bone cancer imaging and treatment (Morigi et al., 2012 (2012).). In other study, Oliveira & coworkers published the nano-MDP labelled with technetium-99 m for bone cancer imaging. They claimed that pharmaceuticals in nanoscale create a new way in oncology (Coelho et al., 2015). Synthesis procedure of the citric acid based PEG dendrimer-G_2 and conjugation with alendronate is illustrated in Fig. 1. To confirm the synthesis of the dendrimer-G_2 and its conjugation to alendronate, FT-IR spectroscopy was done and is shown in Fig. 2. FT-IR of dendrimer-G_2 showed the bands, which are located in the 3430, 2924, and 1726 cm^{-1} wavelengths, related to O-H, C-H, and C = O groups, respectively. FT-IR of the bare alendronate presented the P-O and P = O at 914 and 1140 cm^{-1} respectively. FT-IR of the dendrimer-G_2-alendronate showed all peaks are observed in the dendrimer-G_2 spectrum. Also, the decrease in P-O, P = O and C = O peaks intensity and absorbance confirmed the conjugation of alendronate with dendrimer-G_2. The size and surface morphology of the dendrimer-G_2-alendronate was confirmed by transmission electron microscopy (TEM) analysis (Fig. 3). The TEM image exhibited that the particles were spherical in shape, uniform and monodisperse size distribution. Furthermore, the mean particle size of synthesized dendrimer-G_2-alendronate was about 15 nm. After that, the energy X-ray diffraction mapping (EDS-mapping) analysis was employed to illustrate elemental compositions that are located throughout the dendrimer-G_2-alendronate. As shown in Fig. 4, the elemental compositions of dendrimer-G2-alendronate consist of carbon (C), oxygen (O), nitrogen (N), and phosphorous (P). Fig. 5 shows the evaluation of cell viability of dendrimer-G_2-alendronate on HEK-293 normal cell lines at different concentrations (5, 15, 25, 50, 100, 250, 500, 1000 μg/mL) after 24 h. Statistical analysis showed no cytotoxicity for dendrimer-G_2-alendronate at 24 h compare to the untreated control group.

Amount of dendrimer-G_2-alendronate, amount of reducing agent, and time are different factors that affect the radiolabeling yield. In this study, Box-Behnken software was used to determine these parameters (Table 1a). For the computational study, amount of time, dendrimer-G_2-alendronate, and reducing agent were examined between 5 and 35 min, 10 to 20 mg, and 1 to 4 mg, respectively. Pluses and minuses represent the direct and indirect relation. Fig. 6 shows the effect of two-term interactions in the average mean of the third term by 2D and 3D images. As it is noticeable in 2D, and 3D images, variation is indicated by variation in color. Blue shows the lowest and red shows the highest variation. Thus, the optimal amount of variables were calculated and indicated in Table 1b.

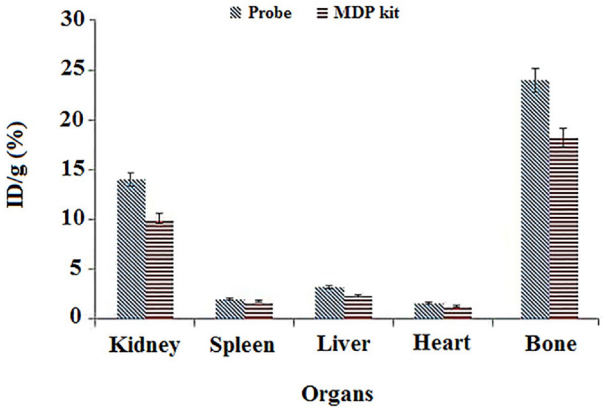

Fig. 8 Biodistribution of ^{99m}Tc-dendrimer-G_2-alendronate and ^{99m}Tc-MDP. Y-axis shows the percentage of ID/g of ^{99m}Tc-dendrimer-G_2-alendronate and ^{99m}Tc-MDP in each organ.

The lyophilized kit was prepared with 12.3 mg dendrimer-G_2-alendronate, 1 mg stannous chloride in the presence of acid ascorbic. ^{99m}Tc-dendrimer-alendronate prepared after adding the 300 MBq of technetium-99 m and shaking for 25 min.

SPECT imaging was done to investigate the accumulation of ^{99m}Tc-dendrimer-G_2-alendronate. ^{99m}Tc-MDP was used as a control group due to its application in the nuclear medicine center as a frequent bone scan agent. 37 MBq of ^{99m}Tc-dendrimer-G_2-alendronate and ^{99m}Tc-MDP were injected through the tail vein. Fig. 7 shows the SPECT images of both radiotracers. As it is evident, ^{99m}Tc-dendrimer-G_2-alendronate showed better accumulation in the skeletal in comparison to ^{99m}Tc-MDP. Same as ^{99m}Tc-MDP, critical organs of the ^{99m}Tc-dendrimer-G_2-alendronate are kidneys and bladder. This means that the urinary system is a significant route in the excretion of ^{99m}Tc-dendrimer-G_2-alendronate. For further investigation, a biodistribution study was done, and results showed the acceptable and more uptake of nano-radiotracer in skeletal in comparison to ^{99m}Tc-MDP. Same as ^{99m}Tc-MDP, high accumulation in kidneys state the main excretion route of nano-radiotracer (Fig. 8). Conjugation of alendronate to citric acid dendrimer led to more solubility of the alendronate. Although more studies need to be done to understand all the aspects of this novel radiotracer, it can be good nano-radiopharmaceuticals to bone cancer at early stage.

4. Conclusion

In this work, we synthesize the citric acid based PEG dendrimer-G_2, and conjugation with alendronate. The FT-IR and TEM confirmed the synthesis of products. MTT assay showed no significant cytotoxicity on HEK-293 at different concentrations. Radiolabeling parameters were optimized by computational study and radiolabeling yield was about 94 percent. SPECT imaging was done for ^{99m}Tc-dendrimer-alendronate and ^{99m}Tc-MDP as a control group. Data showed a high accumulation of nano-radiotracer compared to ^{99m}Tc-MDP. The biodistribution pattern of nano-radiotracer was similar to ^{99m}Tc-MDP.

Declaration of Competing Interest

The authors declare that they have no known competing financial interests or personal relationships that could have appeared to influence the work reported in this paper.

Acknowledgement

Tehran University of Medical Sciences supported this study. The authors wish to thank all the technicians who provided support during the experiments (IR.TUMS.TIPS.REC.1399.166).

References

Sim, S., Wong, N.K., 2021. Biomed. Rep. 14, 42.
J.K. Patra, G. Das, L.F. Fraceto, E.V.R. Campos, M.d.P. Rodriguez-Torres, L.S. Acosta-Torres, L.A. Diaz-Torres, R. Grillo, M.K. Swamy, S. Sharma, S. Habtemariam, H.-S. Shin, Journal of Nanobiotechnology 16 (2018) 71.
Shirzadi-Ahodashti, M., Mortazavi-Derazkola, S., Ebrahimzadeh, M. A., 2020. Surf. Interfaces 21, 100697.
Ebrahimzadeh, M.A., Hashemi, Z., Mohammadyan, M., Fakhar, M., Mortazavi-Derazkola, S., 2021. Surf. Interfaces 23, 100963.
Ahmadi, S., Rahdar, A., Igwegbe, C.A., Mortazavi-Derazkola, S., Banach, A.M., Rahdar, S., Singh, A.K., Rodriguez-Couto, S., Kyzas, G.Z., 2020. Polyhedron 190, 114792.
Murthy, S.K., 2007. Int. J. Nanomed. 2, 129.
Shirzadi-Ahodashti, M., Ebrahimzadeh, M., Ghoreishi, S.M., Naghizadeh, A., Mortazavi, S., 2020. Appl. Organomet. Chem. 34.
Naghizadeh, A., Mizwari, Z.M., Ghoreishi, S.M., Lashgari, S., Mortazavi-Derazkola, S., Rezaie, B., 2021. Environ. Technol. Innov. 23, 101560.
Su, S., Kang, P.M., 2020. Pharmaceutics 12, 837.
Ventola, C.L., 2017. P T 42, 742.
Resnik, D.B., Tinkle, S.S., 2007. Contemp. Clin. Trials 28, 433.
Barrett, T., Ravizzini, G., Choyke, P.L., Kobayashi, H., 2009. IEEE Eng. Med. Biol. Mag. 28, 12.
Svenson, S., Tomalia, D.A., 2005. Adv. Drug Deliv. Rev. 57, 2106.
Jain, K., Kesharwani, P., Gupta, U., Jain, N.K., 2010. Int. J. Pharm. 394, 122.
Wu, M., Shu, J., 2018. Contrast Media & #x26. Mol. Imaging 2018, 1382183.
Gomes, C.M., Abrunhosa, A.J., Ramos, P., Pauwels, E.K.J., 2011. Adv. Drug Deliv. Reviews 63, 547.
Porras, A.G., Holland, S.D., Gertz, B.J., 1999. Clin. Pharma. 36, 315.
Heindel, W., Gübitz, R., Vieth, V., Weckesser, M., Schober, O., Schäfers, M., 2014. Dtsch. Arztebl. Int. 111, 741.
Simon, T.R., Carrasquillo, J.A., Fejka, R., Der, M., 1990. Int. J. Radiat. Appl. Instru. Part B. Nucl. Med. Biol. 17, 793.
Davis, M.A., Jones, A.G., 1976. Semin. Nucl. Med. 6, 19.
Ren, H., Chen, S., Jin, Y., Zhang, C., Yang, X., Ge, K., Liang, X.-J., Li, Z., Zhang, J., 2017. J. Mater. Chem. B 5, 1585.
Patricio, B.F., Albernaz Mde, S., Sarcinelli, M.A., de Carvalho, S.M., Santos-Oliveira, R., Weissmüller, G., 2014. J. Biomed. Nanotechnol. 10, 1242.
Ardestani, M.S., Bitarafan-Rajabi, A., Mohammadzadeh, P., Mortazavi-Derazkola, S., Sabzevari, O., Azar, A.D., Kazemi, S., Hosseini, S.R., Ghoreishi, S.M., 2020. Bioorg. Chem. 96, 103572.
Amin, K.C., Saha, G.B., Go, R.T., 1997. J. Nucl. Med. Technol. 25, 49.
Ciobanu, C.S., Massuyeau, F., Constantin, L.V., Predoi, D., 2011. Nanoscale Res. Lett. 6, 613.
Morigi, V., Tocchio, A., Bellavite Pellegrini, C., Sakamoto, J.H., Arnone, M., Tasciotti, E., 2012. J. Drug Deliv. 2012.
Coelho, B.F., de Souza Albernaz, M., Iscaife, A., Moreira Leite, K.R., de Souza Junqueira, M., Bernardes, E.S., da Silva, E.O., Santos-Oliveira, R., 2015. Curr. Cancer Drug Targets 15, 445.